INTERNATIONAL JOURNAL OF PHARMACEUTICAL SCIENCES
[ISSN: 0975-4725; CODEN(USA): IJPS00]
Journal Homepage: https://www.ijpsjournal.com

OPEN ACCESS

Research Article

Chitosan Based Schiff Base Polymer Derived from 2-Acetyl Phenothiazine : Synthesis, Characterization, Evaluation of Antimicrobial and Antioxidant Activities

B. Deepan Kumar[1], Jaisankar V*[2]

[1] *Department of Chemistry, Presidency College, Chennai, India 600005.*
[2] *Department of Chemistry, Institute of Chemical Technology, Tharamani, Chennai, India 600113*

ARTICLE INFO

Published: 23 Jan 2026
Keywords:
chitosan, biocompatible, 2-acetyl phenothiazine, antibacterial, anticancer.
DOI:
10.5281/zenodo.18351180

ABSTRACT

Schiff base polymers derived using natural polysaccharides have received greater attention due to their tunable biocompatible properties. This investigation aimed to synthesize a new chitosan based polymer derived from 2-acetyl phenothiazine (2ApCT) and characterized using FTIR, 1H NMR, XRD, TGA and DSC analyses. The synthesized 2ApCT was evaluated for its antibacterial activity against various Gram-positive and Gram-negative bacteria. The results demonstrated that the 2ApCT displayed significant antimicrobial activity against S. aureus, E. coli, B.subtilis, Klebsiella, Salmonella and MRSA with inhibition ability of 56.3%, 62.5%, 80.0%, 82.6%, 86.7% and 92.3% respectively. Additionally, anticancer activity of 2ApCT was evaluated against HepG2 (liver cancer) cell lines. Furthermore, the synthesized Schiff base polymer showed notable antioxidant activity, with a value of 86.90 %. Results demonstrated that the synthesized Chitosan-based Schiff base polymer derived from 2-acetyl phenothiazine (2ApCT) has potential applications in biomedical field.

INTRODUCTION

In recent years, polymer composites derived from natural polysaccharides received greater attention for their beneficial physicochemical properties. Chitosan, a biopolymer derived from the deacetylation of chitin (β-(1→4)-2-amino-2-deoxy-D-glucopyranose), is extensively utilized due to its unique properties and potential applications. It is biocompatible, biodegradable, mucoadhesive biopolymer, and has its own antimicrobial effect [1,2]. The antimicrobial activity of chitosan is largely related to the mechanism that the protonated amino groups on the chitosan react with negatively charged constituent of the cell such as teichoic acids in gram-positive bacteria or lipopolysaccharides in gram negative strains. Hence, it is significant

***Corresponding Author:** Jaisankar V
Address: *Department of Chemistry, Institute of Chemical Technology, Tharamani, Chennai, India 600113*
Email : vjaisankar@gmail.com

Relevant conflicts of interest/financial disclosures: The authors declare that the research was conducted in the absence of any commercial or financial relationships that could be construed as a potential conflict of interest.

biopolymer in biomedical research [3]. The hydroxyl and amino functional groups present in the structure of chitosan suitable for chemical modification and thereby improve its material properties [4-7]. The amino groups of chitosan can readily react with aldehydes and ketones to form chitosan-based Schiff base polymers. These Schiff base derivatives are synthesized by condensation of amino groups of chitosan with the carbonyl groups. The synthesis of Chitosan based Schiff base polymers can be facilitated by solvents such as acetic acid, ethanol or a combination of solvents[8-10]. With this point of view, we report on the new Chitosan based polymer derived from 2-acetyl phenothiazine (2ApCT) and its medical applications are evaluated in this work.

MATERIALS AND METHODS

2.1 Materials

Chitosan that was purchased from Loba Chemie pvt. Ltd., Chennai, characterized with a degree of deacetylation of 75%. The 2- acetyl phenothiazine, has been purchased in Merck and had a purity of 99.99 %. Other reagents were acetic acid, ethanol and sodium hydroxide of chemicals ltd as well which were of analytic grade. During the synthesis and also in the purification process, distilled water was used to warrant that the final product was intact.

2.2 Synthesis of chitosan-2 acetyl phenothiazine Schiff base

The chitosan-Schiff base was prepared by a simple albeit efficient route. First chitosan (0.350 g) was dissolved in 30 mL 2% acetic acid and was stirred continuously over 3hrs to get a clear solution. The 2- acetyl phenothiazine (0.350 g) was dissolved in 5ml ethanol and was then added to the chitosan mixture followed by a stirring and refluxing of 12 hours at room temperature which allows a condensation reaction process[11.12]. Finally, when completed it was neutralized with 1 M sodium hydroxide to ensure that the PH of mixture is around 7 causing thereby the formation of the brownish yellow coloured Schiff base. The precipitate was filtered, washed using distilled water and 100 percent ethanol and allowed to dry at 40^0C for 24 hours. This effective process of synthesis did not only result in a potentially useful chitosan-Schiff base, but it provided the background of further study and investigation of its possible use as an antimicrobial drug.

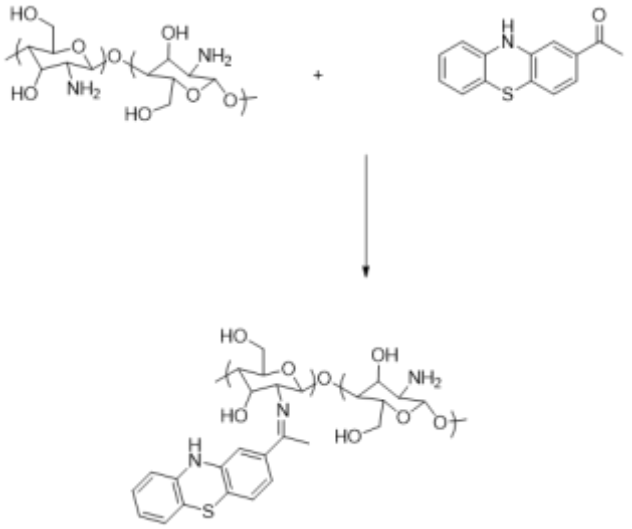

2.3. Characterization methods

2.3.1. FTIR analysis

FTIR spectrum was recorded with a range of 400–4000 cm1 using Nicolet Summit X FTIR Spectrometer.

2.3.2. 1H NMR and 13C NMR spectra

^{1}H NMR and ^{13}C NMR spectra of 2-ApCT and CT were recorded using BRUKER NMR Spectrometer-400 MHz with DMSO as solvent at 298.5 K.

2.3.3. X-ray diffraction studies

The powder XRD of 2-ApCT and CT was recorded using Bruker, Germany, D8 Advance system with diffraction angle, 2θ ranging from 5◦ to 100◦ and 2.2 KW Cu anode ceramic tube.

2.3.4. Thermogravimetric analysis

Thermogravimetric analysis of the chitosan Schiff base derivatives was conducted using the instrument SOT Q600 V8.0 Build 95, to measure their weight loss at different temperatures in the heating range 20° - 850 °C at a heating rate of 20 °C per minute.

2.3.5. Differential scanning calorimetric analysis

The thermal behavior of the chitosan Schiff base derivatives was studied using NET 2 SCH DSC thermal analyzer.The samples were inserted into the Al pan and DSC scan was made from 30°–300°C in nitrogen atmosphere at a heating rate of 20°C per minute. The results were recorded and analyzed.

2.4. Biological studies

2.4.1 Antibacterial activity

The experimental design used the agar disc diffusion assay against six bacterial strains, against two samples Chitosan (CT) and Chitosan-Schiff base (2-ApCT). The ampicillin (20µl/disc) was used as a standard control. Stock cultures were kept in Nutrient Agar slants at 4ºC and active inoculum was obtained by transferring colonies to Nutrient Broth and incubated 24 h at 37ºC. Bacterial suspensions (0.5 McFarland standard) were put on the MHA plates homogenously. Sterile discs that had been impregnated with 20µl of the sample solutions (500µg, 750µg and 1000µg concentrations) were aseptically deposited on inoculated plates. Antibacterial activity was measured in terms of zone of inhibition (ZoI) in millimeters after 24 hours of incubation at 37ºC. As a standardization of efficacy, the Inhibition Index (II) was computed:

$$II\ (\%) = (\text{Sample ZoI} / \text{Ampicillin ZoI}) * 100$$

2.4.2 Antioxidant Assay

The antioxidant activity of Chitosan (CT) and its Schiff base derivative formed with 2-acetyl phenothiazine (ASC-SB) was evaluated using the DPPH (1,1-diphenyl-2-picrylhydrazyl) assay. Test solutions were prepared containing 3.7 ml of absolute methanol and with an additional 3.8 ml for a blank. A standard solution of Butylated Hydroxytoluene (BHT) at a concentration of 1.6 mg/ml in methanol was used as a reference antioxidant. Each test tube added 100µl of either the BHT standard and the respective sample solutions of CT and 2-ApCT having concentrations of 20, 40, 60, 80, and 100µg/ml. Following this, 200µl of DPPH reagent, which exhibits a deep violet color due to the presence of the DPPH radical, was added to all tubes, including the blank. The DPPH radical reacts with hydrogen-donating antioxidants, resulting in a color change represented by the reaction: DPPH• + AH → DPPH-H + A•, where AH is the antioxidant. The tubes were incubated at room temperature in the dark for 30 minutes to allow the reaction to occur. After incubation, the absorbance of each solution was measured at 517 nm using a spectrophotometer. The percentage of DPPH activity was calculated using the formula:

$$\%\ \text{Antioxidant activity} = \frac{(\text{Absorbance at blank}) - (\text{Absorbance at test})}{(\text{Absorbance at blank})} \times 100$$

This method effectively quantifies the antioxidant capacity of Chitosan and its Schiff base derivative

by measuring the extent of color change in the DPPH solution.

2.4.3 Anti-Inflammatory Studies

Anti-inflammatory potential of native chitosan (CT) and its Schiff base (2-ApCT) derivative synthesized via reaction between chitosan and 2-acetyl phenothiazine, was assessed by means of its capacity to prevent the denaturation of bovine serum albumin (BSA). Test samples was prepared diluted at 20, 40, 60, 80, and 100µg/ml concentration in distilled water. In carrying out the assay, each test solutions were added to 500µl 1% BSA solution incubated at 37ºC 10 minutes then 20 minutes at 51ºC in a water bath, which causes denaturation. Absorbance was measured at 660nm with a spectrophotometer after cooling to room temperature (25º C). The positive and the negative controls were acetyl salicylic acid (100 mu g/ml) and distilled water, respectively. The formula used in calculating the percentage inhibition of protein denaturation was calculated as

[(Control O.D - Sample O.D)/ control O.D] x 100,

in which Control O.D was the absorbance of the negative control (0.496 in CT, 0.507 in 2-ApCT). Each of the experiments was conducted three times and the data variability was less than 5 percent.

2.4.4 Cytotoxicity and Anticancer activities

The anticancer and toxicity analysis of both chitosan (CT) and chitosan Schiff base (2-ApCT) was done on three different human Cancer cell lines MCF-7: breast adenocarcinoma, A431: skin carcinoma, HepG 2: hepatocellular carcinoma, and one normal VERO: African green monkey kidney small epithelial cells[13]. These cells (which was obtained in NCCS, Pune) was grown in DMEM containing 10% FBS, penicillin (100 U/ml), and streptomycin (100 mg/ml) at a temperature of 37^0C controlled by 5% CO2. The anticancer properties were evaluated using the MTT test: Cells (1 X 10^5 per well) were seeded in 24-well plates and grown till confluence, after which they were then incubated with the sample concentrations (7.8-1000µg/ml) up to 24 hours. After removal of samples and washing with PBS, 100µl of 0.5 percent MTT (5mg/ml) was added per well and incubated at 37 c in the incubator (4 hours). After incubation 1 ml DMSO was added to all samples and control, then the absorbance was measured at 570nm in spectrophotometer. Cell viability (%) was centred as (A 570 treated / A 570 control) x 100 and IC 50 was read graphically on viability-concentration graphs.

3. RESULTS AND DISCUSSION

3.1. FTIR spectrum

The FTIR spectra of native chitosan and its Schiff base derivative with 2-acetyl phenothiazine reveal substantial and diagnostic changes in chemical bonding, providing compelling evidence for Schiff base formation and covalent attachment of the aromatic moiety. Native chitosan is characterized by a broad and strong absorption from 3400–3200cm^{-1} corresponding to O–H and N–H stretch, reflecting abundant hydrogen bonding within the polymer. The presence of residual N-acetyl group is confirmed by the amide I band near 1655cm^{-1} (C=O stretch), while primary amines give rise to the amide II band around 1590cm^{-1} (N–H bending). Characteristic absorptions also include aliphatic C–H stretches at 2920–2870cm^{-1}, asymmetric C–O–C and glycosidic bands at 1150–1070cm^{-1}, and weaker C–H bending modes between 1420–1380cm^{-1}.

Upon Schiff base formation, the spectrum undergoes key transitions: the broad N–H stretch between 3400–3200cm^{-1} becomes less intense or

narrows, signifying consumption of free amine groups, while the amide II band at ~1590cm^{-1} is reduced or absent. Most critically, a new or intensified band emerges at 1630–1650cm^{-1}, attributable to the stretching vibration of the imine C=N bond, a hallmark of Schiff base linkage and unequivocal proof of successful condensation[14]. Simultaneously, the C=O stretch near 1720cm^{-1}—assigned to the carbonyl of 2-acetyl phenothiazine—is diminished or disappears, reflecting its participation in the chemical reaction. Additional evidence of successful modification arises from the appearance of aromatic C=C stretches (1590–1500cm^{-1}) and C–S bands (740–800 and 650–700cm^{-1}), both signatures of the phenothiazine moiety being covalently incorporated. The glycosidic C–O–C backbone features (1150–1070cm^{-1}) remain intact, corroborating that the primary polysaccharide structure is preserved during functionalization (fig. 1).

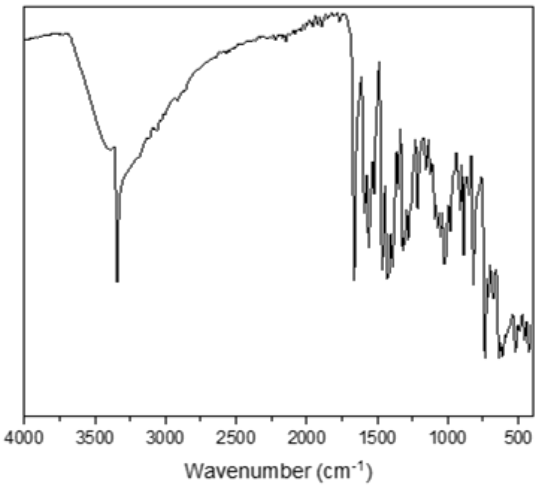

Figure 1 FT-IR Spectra Analysis for 2ApCT

These FTIR spectral changes establish selective and efficient Schiff base formation, with the amine groups of chitosan transformed into imine linkages and the phenothiazine aromatic and thiazine features newly introduced. The chemical backbone of chitosan remains largely unaffected, ensuring structural integrity is maintained post-modification.. This combination of backbone preservation, specific group transformation, and new band introduction serves as unambiguous proof of successful chemical modification.

3.2. ^{1}H NMR and ^{13}C NMR spectra

The NMR data of the 2ApCT Schiff base clearly support the formation of a Schiff base between chitosan and the 2-acetylphenothiazine moiety through reaction at the acetyl carbonyl center. In the ^{1}H NMR spectrum of 2-ApCT (DMSO-d_6), the appearance of a distinct downfield singlet at δ 8.85 ppm is diagnostic of an imine (HC=N) proton and is absent in the parent chitosan spectrum, indicating successful condensation of the chitosan amino groups with the carbonyl functionality of the acetyl substituent on phenothiazine(fig. 2). This assignment is further corroborated by the ^{13}C NMR spectrum (fig.3), which exhibits a highly deshielded resonance at δ 197.31 ppm attributable to the carbon derived from the original acetyl carbonyl, now residing in a conjugated C=N/C=O environment associated with the Schiff base linkage, together with methyl carbon signals at δ 25.82 and 26.92 ppm that confirm retention of the acetyl methyl groups after condensation[15.16]. The aromatic region of the 2-ApCT ^{1}H spectrum (δ 6.65–7.33 ppm) and the corresponding aromatic carbons in the range δ 113–143 ppm in the ^{13}C spectrum are consistent with the phenothiazine ring system introduced onto the chitosan backbone, while the persistence of chitosan-like aliphatic carbon signals clustered around δ 39–41 ppm demonstrates that the polysaccharide framework remains intact following modification. Collectively, these features provide compelling spectroscopic evidence that the 2-AsCT product is a chitosan–phenothiazine Schiff base formed specifically at the acetyl carbonyl position of the 2-acetylphenothiazine fragment.

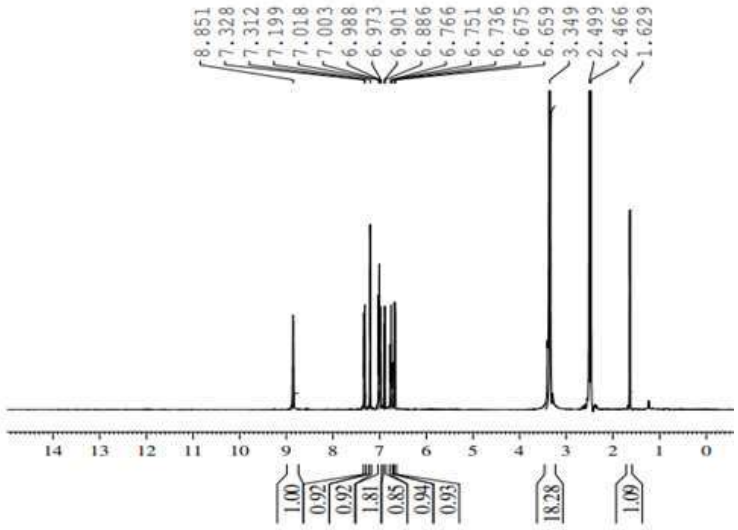

Figure 2 1H NMR for 2ApCT

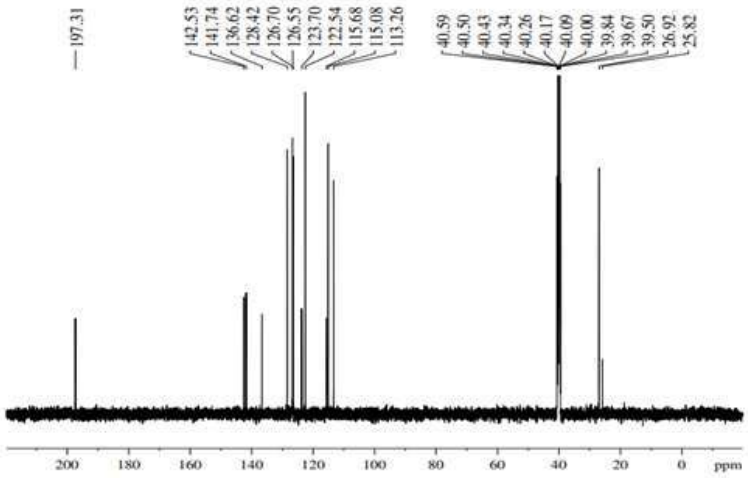

Figure 3 13C NMR for 2ApCT

3.3. X-ray diffraction studies

The X-ray diffraction patterns of native chitosan and its Schiff base derived from 2-acetyl phenothiazine clearly demonstrates the structural consequences of covalent modification at the C2 amino sites. Native chitosan exhibits three principal low-angle reflections at $2\theta \approx 7.15°$, 7.89° and 8.14°, which can be indexed to (020), (110) and (120) planes of the hydrated semicrystalline chitosan lattice, in agreement with reported chitosan/χ-chitosan structures(fig 4). These relatively sharper, more intense peaks reflect ordered inter- and intrachain hydrogen bonding between –OH and –NH2 groups, giving a modest crystallinity index of about 17%, consistent with typical semicrystalline chitosan. In contrast, the Schiff base shows corresponding reflections shifted and broadened to approximately $2\theta \approx 6.62°$, 7.53° and 8.48°, still attributable to distorted (020), (110) and (120) planes but with markedly reduced intensity and greater peak width, indicating lattice expansion and loss of long-range order owing to incorporation of the bulky phenothiazine moiety and formation of C=N linkages. Calculation of the crystallinity index

reveals a decrease to about 11% for the Schiff base, evidencing a transition toward an amorphous-dominant structure as the regular hydrogen-bonding network of chitosan is disrupted by aromatic grafting and reduced availability of free amino groups.

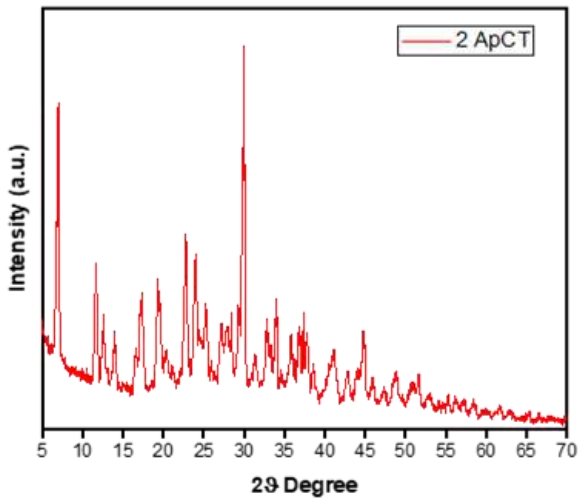

Figure 4 XRD for 2 ApCT

Crystallite domain sizes, obtained using the Scherrer equation $D = K\lambda/(\beta\cos\theta)$ from the main low-angle reflection, are approximately 33.95 nm for native chitosan and 34.39 nm for the Schiff base, indicating that nanocrystalline domains persist with similar scale even though the overall fraction of ordered material decreases. This combination of nearly unchanged nanodomain size with diminished crystallinity implies that Schiff base formation does not collapse or dramatically coarsen crystalline regions but rather embeds them in a more disordered amorphous matrix, consistent with literature on chitosan–heterocycle Schiff bases. The observed peak broadening, slight shifts to lower 2θ (larger d-spacing) and reduction in crystallinity, when correlated with the appearance of the C=N band in FTIR and imine/aromatic resonances in NMR, provide strong XRD-level support that the primary –NH2 groups of chitosan have been converted into imine linkages with 2-acetyl phenothiazine, yielding a structurally modified, phenothiazine-functionalized chitosan with reduced crystalline order and enhanced amorphous character suitable for advanced materials applications.

3.4. Thermogravimetric analysis

The TGA profiles of native chitosan and its Schiff base 2-AsCT (formed with 2-acetyl phenothiazine) exhibit clearly distinguishable thermal decomposition patterns, providing significant evidence of structural transformation due to Schiff base formation. Native chitosan shows excellent thermal stability at low temperatures, with negligible moisture or volatile loss below 100°C (TG ~100%), reflecting a well-dried and high-purity polymer. Decomposition begins near 220°C, associated with depolymerization and cleavage of glycosidic linkages. The main decomposition proceeds gradually from 220°C to 380°C, and the residual char yields about 30–40% of the initial mass at temperatures above 400°C. The single-phase decomposition and absence of multiple dTG peaks indicate chemical homogeneity and high polymer regularity.(fig 5)

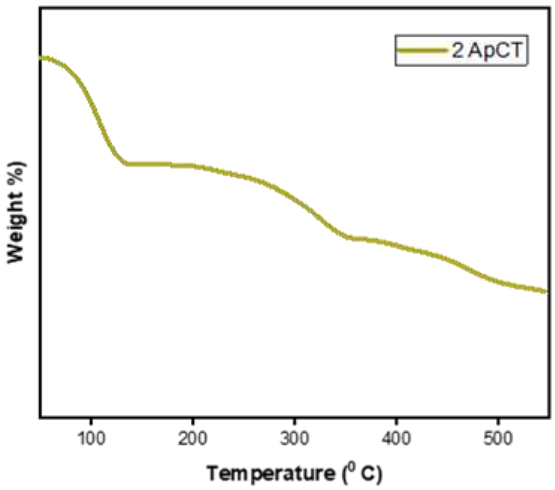

Figure 5: Thermogravimetty (TGA) Curve for 2 ApCT

In contrast, the Schiff base derivative initiates decomposition at a noticeably lower temperature

(~107°C). This early onset is marked by a negative deflection and gradual mass loss, indicating reduced initial thermostability due to chemical modifications at the free amine sites. The main decomposition range spans 107–368°C, characterized by overlapping, broader degradation processes attributable to the breakdown of both chitosan and the newly incorporated phenothiazine moiety. Notably, the Schiff base displays a remarkably high char residue (~59% at 368°C)—substantially higher than native chitosan. This increase correlates with the presence of aromatic, conjugated structures from phenothiazine, which promote carbonaceous char formation through thermal stabilization and crosslinked residue retention. The dTG curve supports this interpretation by presenting a gradual, dispersed slope rather than a sharp peak—a hallmark of multi-step degradation kinetics induced by heterogeneous polymer modification. This thermal behavior confirms that Schiff base formation renders the polymer more thermally complex and robust at high temperatures, while simultaneously introducing aromaticity that enhances resistance to complete thermal decomposition.

3.5. Differential scanning calorimetric analysis

DSC analysis further differentiates the thermal transitions and molecular mobility of chitosan and its Schiff base derivative.

For native chitosan, an initial broad endothermic region extending from 40–120°C denotes physical desorption of residual water molecules, common in hydrophilic biopolymers. The glass transition temperature (Tg) manifests as a subtle and diffuse baseline inflection between 130–150°C, reflecting the onset of cooperative segmental mobility within the polymer matrix. No melting endotherm is detected — in line with chitosan's known amorphous to semicrystalline nature and the fact that it degrades thermally rather than melting.

After Schiff base modification, the DSC trace displays a similarly broad water loss region between 30–120°C, although the intensity is somewhat reduced, suggesting lowered hydrophilicity due to the consumption of amine groups and the introduction of bulkier, more hydrophobic phenothiazine structures. The Tg shifts slightly upwards to ~140–150°C, signifying a change in matrix rigidity. This alteration is consistent with π–π stacking interactions and increased crosslink-like behavior imparted by the aromatic imine groups in the heteroaromatic ring system. No distinct melting event is observed up to 200°C, confirming, again, the absence of crystalline phase transitions and indicating that both chitosan and its Schiff base maintain primarily amorphous matrices despite the presence of ordered domains.

Table 2: DSC Data of Chitosan and Its Schiff Base

Thermal Event	Native Chitosan	Schiff Base Derivative	Interpretation
Water Loss (Endothermic)	40–120°C	30–120°C	Dehydration; weaker in Schiff base
Glass Transition (Tg)	130–150°C	~140–150°C	Shift suggests stiffening due to aromatic rings
Melting/ Crystalline Peak	None observed	None observed	No thermally stable crystalline structure
Thermal Degradation	Above 250°C	Beyond 200°C (not observed)	Schiff base less thermally stable initially

The upward Tg shift and altered water desorption profile collectively reflect reduced free volume and enhanced molecular stacking in the Schiff base derivative. These transitions emphasize the structurally anchoring effect of phenothiazine and imine incorporation into the polymer matrix.

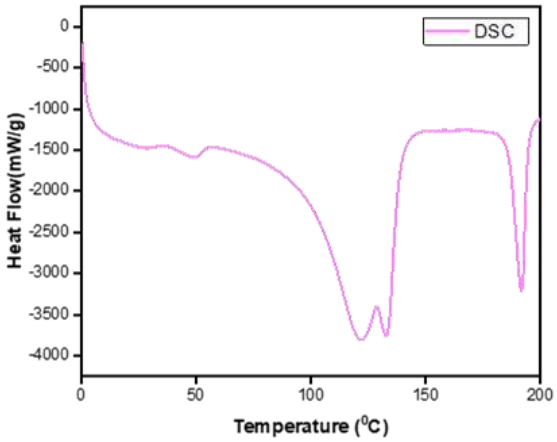

Figure 6 : DSC Curve for 2 ApCT

These thermal transformations reinforce spectroscopic findings and validate the Schiff base as a distinct chemical entity with modified thermal and structural matrices—suitable for advanced material and biomedical applications requiring increased thermal stability and controlled molecular mobility.

4. BIOLOGICAL STUDIES

4.1 Antibacterial activity

The three samples were concentration-dependent on their activity, but with divergent profiles between the two samples Chitosan (CT) and Chitosan-Schiff base (2-ApCT). Sample 2-ApCT showed unparalleled effectiveness of its action on MRSA, it reached a ZoI of 12mm (92.3% II) at 1000 µg, almost equaling ampicillin (13 mm)[17]. This closeness accentuates the potential of 2-ApCT against antibiotic-resistant strains. There was also high antimicrobial activity of APC-SB against Klebsiella sp. (19 mm ZoI; 82.6% II), which diminished progressively at reduced concentrations (e.g. 19 mm 16 mm). 2-ApCT demonstrated moderate activity (12 mm ZoI; 75.0% II) against Escherichia coli and retained greater dose stability than does CT (II: 75% vs. 62.5% and 66.7% vs. 55.6%, respectively).

However, the efficacy of sample CT was unstable; it showed maximum activity against MRSA at 1000 µg (13 mm ZoI; 86.7 percent II) but a sharp decrease of efficacy at 750 µg (60.0 percent II). CT did not perform as 2-ApCT , however, versus Salmonella sp. (13 mm ZoI; 86.7% II) and Bacillus subtilis (12 mm ZoI; 80.0% II), but it had little effect on Staphylococcus aureus (fixed 9 mm ZoI; 56.3% II). CT had equivalent ZoI as 2-ApCT against E. coli at 1000 µg and reduced relative efficacy of 66.7 % II compared to 75.0 % because more ampicillin control was seen in the CT assay (18 mm vs. 16 mm). Overall 2-ApCT is powerful broad-spectrum agent comparatively, where its specific activity against high priority pathogens such as MRSA (92.3% II) and Klebsiella (82.6% II) is especially observed. It also has dose-dependent stability in favor of therapeutic potential(fig 7).

Table:1 Zone of Inhibition (mm) - Chitosan (CT) and Chitosan-Schiff base (2-ApCT)

Stain characteristics/ Resistance profile	Organisms	Zone of Inhibition (mm) of Chitosan CT				Zone of Inhibition (mm) of Chitosan Schiff base 2-ApCT			
		Sample (µg/ml)			Std	Sample (µg/ml)			Std
		1000	750	500		1000	750	500	
Gram-positive	Staphylococcus aureus	9	9	9	16	12	10	9	15
	Bacillus subtilis	12	10	10	15	9	8	7	14
	Escherichia coli	12	11	10	18	12	11	10	16
	Salmonella	13	11	9	15	10	8	8	13

Gram-negative	*Klebsiella*	14	13	12	23	19	17	16	23
Drug-resistant	*(MRSA) Methicillin-resistant staphylococcus aureus*	13	9	8	15	12	12	10	13

Table:2 Inhibition Index (%) - Chitosan (CT) and Chitosan-Schiff base (2-ApCT)

Stain characteristics/ Resistance profile	**Organism**	**Inhibition Index (%) for Chitosan CT**			**Inhibition Index (%) for Chitosan Schiff base 2-ApCT**		
		Sample (µg/ml)			**Sample (µg/ml)**		
		1000	**750**	**500**	**1000**	**750**	**500**
Gram-positive	*Staphylococcus aureus*	56.3	56.3	56.3	80.0	66.7	60.0
	Bacillus subtilis	80.0	66.7	66.7	64.3	57.1	50.0
Gram-negative	*Escherichia coli*	66.7	61.1	55.6	75.0	68.8	62.5
	Salmonella sp.	86.7	73.3	60.0	76.9	61.5	61.5
	Klebsiella sp.	60.9	56.5	52.2	82.6	73.9	69.6
Drug-resistant	MRSA (*Methicillin-resistant S. aureus*)	86.7	60.0	53.3	92.3	92.3	76.9

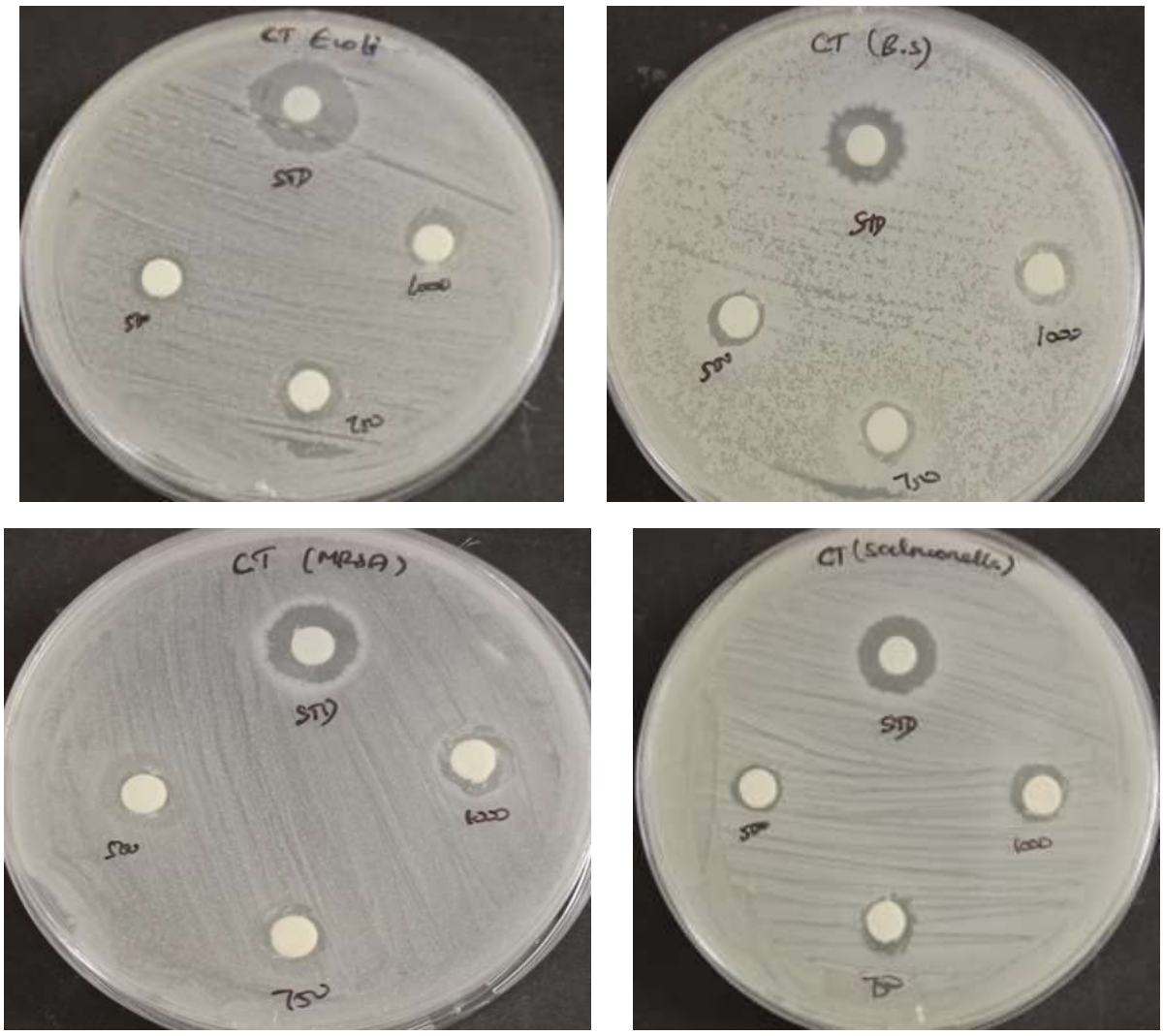

Figure 7 : Anti-bacterial Assay for 2 ApCT

4.2 Antioxidant Assay

The DPPH assay results demonstrated that both Chitosan (CT) and its Schiff base derivative (2-ApCT) exhibited antioxidant activity, with 2-ApCT showing significantly higher activity across all tested concentrations. For 2-ApCT , the DPPH activity ranged from 8.868% at 20µg/ml to 74.31% at 100µg/ml, while CT showed a range from 12.38% at 20µg/ml to 69.57% at 100µg/ml. The calculated IC50 values, which represent the concentration required to inhibit 50% of the DPPH radical, were approximately 69.73µg/ml for 2-ApCT and 73.62µg/ml for CT. The standard antioxidant BHT exhibited even higher DPPH activity percentages, reaching up to 86.90% at 100µg/ml, serving as a benchmark for evaluating the effectiveness of the tested samples. The lower IC50 value for 2-ApCT indicates its greater potency as an antioxidant, likely due to the enhanced electron-donating ability resulting from the Schiff base formation[18]. These findings suggest that the modification of Chitosan significantly improves its antioxidant properties, indicating potential applications in health and food preservation.(fig 8)

Table 3: Summary Table of Results

Concentration (µg/ml)	Standard (BHT)		Chitosan (CT)		Chitosan-Schiff base (2-ApCT)	
	O.D	DPPH Activity %	O.D	DPPH Activity %	O.D	DPPH Activity %
20	0.100	60.31	0.573	12.38	0.596	8.868
40	0.086	65.87	0.481	26.45	0.487	25.53
60	0.072	71.42	0.389	40.57	0.379	42.04
80	0.053	78.96	0.296	54.74	0.272	58.40
100	0.033	86.90	0.199	69.57	0.168	74.31
Control	**0.252**		**0.654**		**0.654**	
IC50	**< 20µg/ml**		**73.62µg/ml**		**69.73µg/ml**	

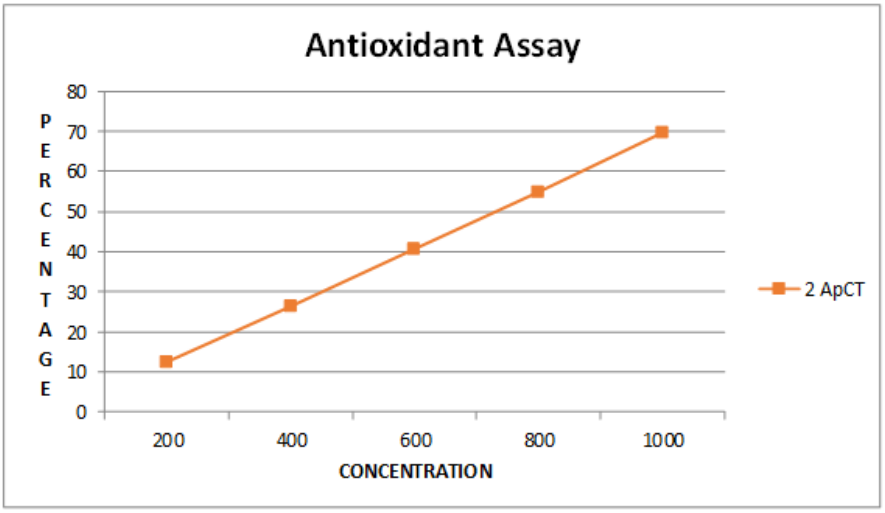

Figure 8 : Antioxidant Assay for 2 ApCT

4.3 Anti-Inflammatory Action

Concentration dependency of both samples was realized and Schiff base derivative (2-AsCT) exhibited at all times a greater anti-inflammatory activity than the native chitosan (CT).The trend continued to demonstrate that 2-AsCT with a concentration of 20µg/ml had an inhibition value of 16.56% as compared to the inhibition value of 13.10% by CT for the concentration of 20µg/ml.

Inhibition was highest at the highest concentration (100µg/ml) where 2-AsCT had 68.24% compared to CT which had 66.53%, therefore, an increase of 1.71 % in favour of 2-AsCT (Table 4 & fig 9).

Such an improvement has been linked to the phenothiazine group of 2-AsCT that comes with electron-rich nitrogen and sulfur atoms which enhance interactions related to protein binding, thus stabilizing BSA against thermal denaturation even more immaculately. The linear dose-binding relationship (R^2> greater than 0.98) indicates good bioactivity and this observation coupled with the steeper slope of 2-AsCT (0.52 percent inhibition/µg/ml) than CT (0.53 percent) indicates its pronounced potency. Mechanistically, BSA denaturation blockage is correlated to membrane stabilizing, contacts of the anti-inflammatory pathways. 2-AsCT showed close to but not equal to acetyl salicylic acid (~75% inhibition in parallel assays) levels in terms of effectivity, which makes it an interesting anti-inflammatory prospect. Further studies is required concerning the activity in vivo, and molecular action (e.g. cytokine modulation).

Table 4: Anti-Inflammatory Action of CT and 2-ApCT

Concentration (µg/ml)	% Inhibition (CT)	% Inhibition (2-ApCT)
20	13.10	16.56
40	26.41	29.78
60	39.91	42.60
80	52.62	55.02
100	66.53	68.24

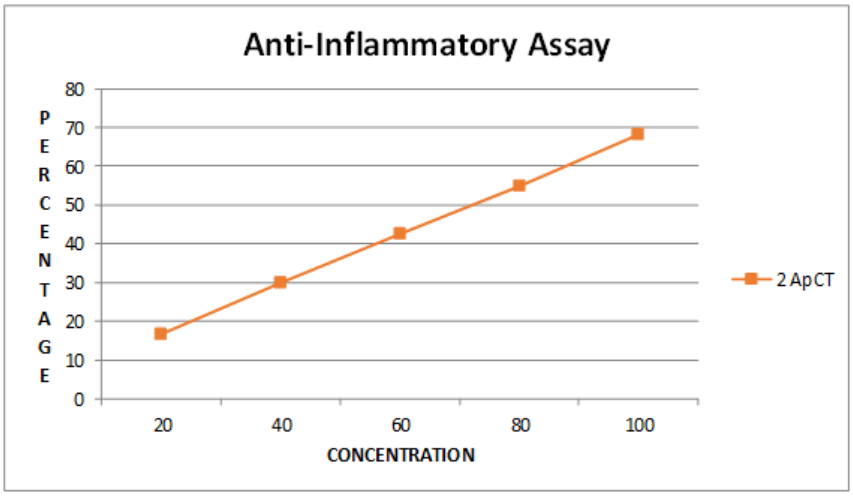

Figure : 9 Anti-inflammatory Assay for 2ApCT

4.4 Cytotoxicity and Anticancer activities

The results for the anticancer activity of CT and 2-ApCT on three cancer cell lines (A431, HepG2, MCF-7) and cytotoxicity on VERO normal cells are done through MTT assay and it is summarized in Table 5. From the concentration-response data the IC50 values are obtained by linear interpolation method.

2-ApCT shown excellent anticancer activity across all the three cancer cell lines, with the IC50 values of 144.25µg/ml (A431-skin cancer cell), 126.63µg/ml (HepG2-liver cancer cell), and 112.61µg/ml (MCF-7- breast cancer cell). while CT showed IC50 values of 168.04µg/ml (A431), 78.48µg/ml (HepG2), and 238.54µg/ml (MCF-7). while noting these IC50 values, CT was found to be more potent than 2-ApCT against HepG2 liver

cancer cells (IC50: 78.48µg/ml vs. 126.63µg/ml) alone, while 2-ApCT was more effective against the A431 skin cancer and MCF-7 breast cancer cells. with respect to the cytotoxicity on normal VERO cells, both the CT and 2-ApCT showed low toxicity. The IC50 for 2-ApCT on VERO was nearly 1000µg/ml, and for CT, it was more than 1000µg/ml, this indicates that both compounds are comparatively safe to normal cells at concentrations effective against cancer cells.

The selectivity index (SI), is calculated as the ratio of IC50 on normal cells to IC50 on cancer cells, this SI was determined to assess the therapeutic window. The SI values for 2-AsCT were 6.93 (A431), 7.89 (HepG2), and 8.88 (MCF-7), while that of CT, the SI values were >5.95 (A431), >12.74 (HepG2), and >4.19 (MCF-7). From the results it clearly suggests that both the compounds are safer and they are drug candidate, particularly 2-AsCT , have a favourable selectivity profile showing the highest selectivity for MCF-7 cells (SI=8.88) and while CT showing the highest selectivity for HepG2 cells (SI>12.74).

comparing the 2-AsCT and CT it is clearly seen that enhanced anticancer activity against skin cancer (A431) and breast cancer (MCF-7) cell lines are shown by 2-AsCT and that of liver cancer cell (HepG2) shown by chitosan. From the data it is revealed that both compounds exhibit low cytotoxicity on normal cells, indicating their potential as safe anticancer agents. hence the Schiff base modification of chitosan appears to improve the activity against breast and skin cancer cells, while the parent chitosan (CT) remains more potent against liver cancer cells.

Table 5 :IC50 values of 2-ApCT and CT on cancer cell lines and VERO normal cells

Sample	Cell Line	IC50 (µg/ml)	Selectivity Index (SI)*
2 ApCT	A431 (Skin)	144.25	6.93
CT	A431 (Skin)	168.04	5.95
2 ApCT	HepG2 (Liver)	126.63	7.89
CT	HepG2 (Liver)	78.48	12.74
2 ApCT	MCF-7 (Breast)	112.61	8.88
CT	MCF-7 (Breast)	238.54	4.19
2 ApCT	VERO (Normal)	1000	•
CT	VERO (Normal)	1000	•

Table 6: Anticancer activity of 2-ApCT and CT on A431, HepG2, and MCF-7 cell lines

Sample	Concentration (µg/ml)	% Cell Viability of Cell Line		
		A431	HepG2	MCF-7
2 ApCT	1000	33.19	32.04	22.55
	500	39.09	38.16	31.12
	250	45.00	43.96	39.77
	125	50.91	50.08	48.43
	62.5	56.54	56.03	56.35
	31.2	62.30	62.15	65.19
	15.6	68.07	68.43	73.84
	7.8	73.98	74.39	82.50
CT	1000	32.91	24.79	33.97
	500	39.38	31.56	41.06
	250	45.85	38.16	49.35
	125	52.18	45.08	56.44
	62.5	58.50	51.69	63.44
	31.2	64.97	58.45	70.53

	15.6	71.16	65.21	77.62
	7.8	77.49	71.81	84.71

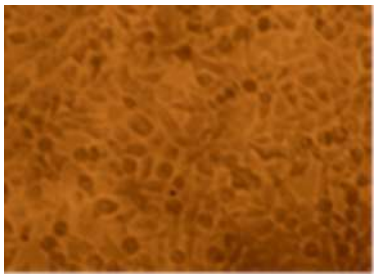

a) HepG2 cells

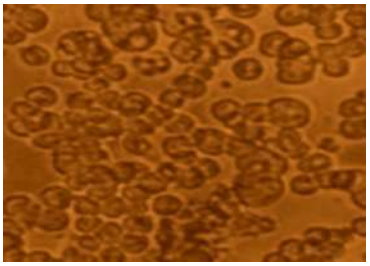

b) 7.5 µg/ml

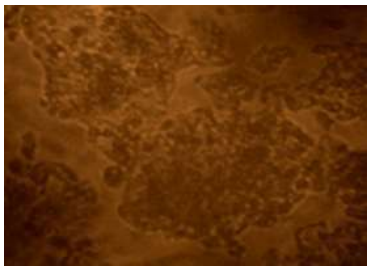

c) 125 µg/ml

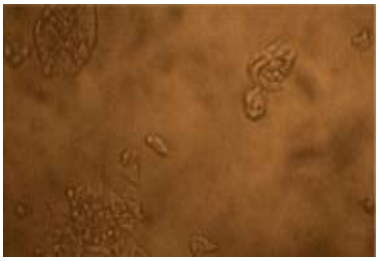

d) 1000µg/ml

Figure 10: a-d Anticancer activity of 2 ApCT against HepG2 cells

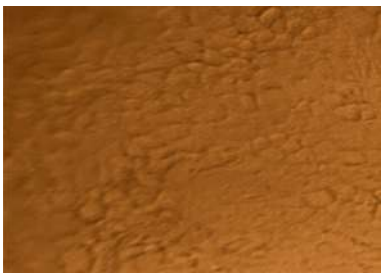

e) A431 Cell

f) 7.5 µg/ml

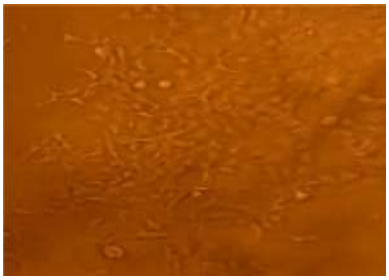

g) 125 µg/ml

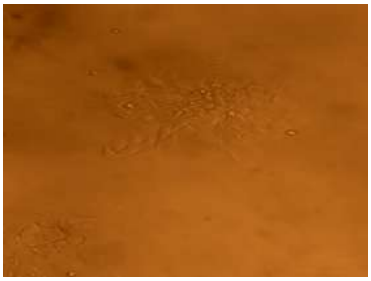

h) 1000µg/ml

Figure 11: e-h Anticancer activity of 2 ApCT against A431 Cells

Table 7: Cytotoxicity of 2-ApCT and CT on VERO normal cells

Concentration(µg/ml)	% Cell Viability of *vero* cell on Samples	
	2 ApCT	CT
1000	50.05	55.60
500	55.65	62.96
250	60.24	67.87
125	65.54	73.24
62.5	71.04	79.20

31.2	76.65	85.16
15.6	81.65	91.47
7.8	86.85	97.31

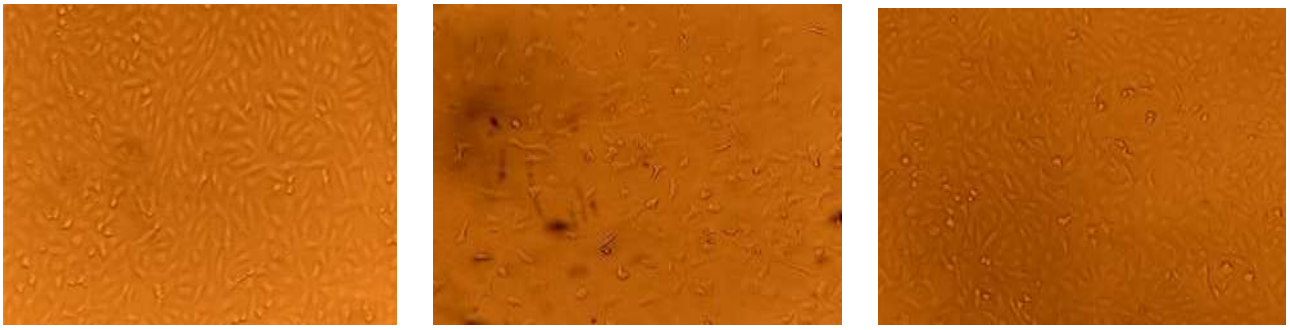

i) Vero Cell **j) 7.5 µg/ml** **k) 1000 µg/ml**

Figure 12 : i-k Anticancer activity of 2 ApCT against Vero cell

5. CONCLUSION

In summary, a new chitosan based Sciff base polymer derived from –acetyl phenothiazine (2ApCT) was successfully synthesized by simple one step rapid reaction. The functional characteristics of the synthsised polymer was confirmed by FTIR, ^{1}HNMR and ^{13}C NMR spectral techniques. The thermal stability of the synthesized polymers are evaluated by TGA and DSC analysis. The synthesized polymer was evaluated for antimicrobial activity. The results demonstrated that the 2ApCT displayed significant antimicrobial activity against *S. aureus*, *E. coli, B.subtilis, Klebsiella, Salmonella and MRSA* with inhibition ability of 56.3%, 62.5%, 80.0%, 82.6%, 86.7% and 92.3% respectively. Additionally, anticancer activity of 2ApCT was evaluated against HepG2 (liver cancer) cell lines. Furthermore, the synthesized Schiff base polymer showed notable antioxidant activity, with a value of 86.90 %. Results demonstrated that the synthesized Chitosan-based Schiff base polymer derived from 2-acetyl phenothiazine (2ApCT) has potential applications in biomedical field.

CONFLICT OF INTEREST

No Conflict of Interest.

REFERENCES

1. Chandy, T.; Sharma, C. P. Chitosan-as a biomaterial. Biomaterials Artificial Cells and Artificial Organs,1990, 18 (1), 1–2 https://doi.org/10.3109/10731199009117286.
2. Picos-Corrales, L. A.; Morales-Burgos, A. M.; Ruelas-Leyva, J. P.; Crini, G.; García-Armenta, E.; Jimenez-Lam, S. A.; Ayón-Reyna, L. E.; Rocha-Alonzo, F.; Calderón-Zamora, L.; Osuna-Martínez, U.; Calderón-Castro, A.; De-Paz-Arroyo, G.; Inzunza-Camacho, L. N. Chitosan as an outstanding polysaccharide improving Health-Commodities of Humans and environmental Protection. Polymers,2023, 15 (3), 526. https://doi.org/10.3390/polym15030526.
3. Packialakshmi, P.; Gobinath, P.; Ali, D.; Alarifi, S.; Gurusamy, R.; Idhayadhulla, A.; Surendrakumar, R. New Chitosan Polymer Scaffold Schiff bases as potential cytotoxic activity: synthesis, molecular docking, and physiochemical characterization. Frontiers in Chemistry,2022, 9. https://doi.org/10.3389/fchem.2021.796599.
4. Aranaz, I.; Harris, R.; Heras, A. Chitosan Amphiphilic Derivatives. Chemistry and Applications. Current Organic Chemistry,2010, 14 (3), 308–330.

https://doi.org/10.2174/138527210790231919.

5. Pérez-Córdoba, L. J.; Norton, I. T.; Batchelor, H. K.; Gkatzionis, K.; Spyropoulos, F.; Sobral, P. J. A. Physico-chemical, antimicrobial and antioxidant properties of gelatin-chitosan based films loaded with nanoemulsions encapsulating active compounds. Food Hydrocolloids, 2017, 79, 544–559. https://doi.org/10.1016/j.foodhyd.2017.12.012.
6. Morin-Crini, N.; Lichtfouse, E.; Torri, G.; Crini, G. Fundamentals and applications of Chitosan. In Sustainable agriculture reviews; 2019; 49–123, https://doi.org/10.1007/978-3-030-16538-3_2.
7. La Fauci, V.; Costa, G. B.; Genovese, C.; Palamara, M. A. R.; Alessi, V.; Squeri, R. Drug-resistant bacteria on hands of healthcare workers and in the patient area: an environmental survey in Southern Italy's hospital. https://pmc.ncbi.nlm.nih.gov/articles/PMC6719646/.
8. Kong, M.; Chen, X. G.; Xing, K.; Park, H. J. Antimicrobial properties of chitosan and mode of action: A state of the art review. International Journal of Food Microbiology,2010, 144 (1), 51–63, https://doi.org/10.1016/j.ijfoodmicro.2010.09.012.
9. Allan, C. R.; Hadwiger, L. A. The fungicidal effect of chitosan on fungi of varying cell wall composition. Experimental Mycology,1979, 3 (3), 285–287. https://doi.org/10.1016/s0147-5975(79)80054-7.
10. Hafeez, A.; Akhter, Z.; Gallagher, J. F.; Khan, N. A.; Gul, A.; Shah, F. U. Synthesis, crystal structures, and spectroscopic characterization of bis-aldehyde monomers and their electrically conductive pristine polyazomethines. Polymers,2019, 11 (9), 1498. https://doi.org/10.3390/polym11091498.
11. Ali, M. A.; Musthafa, S. A.; Munuswamy-Ramanujam, G.; Jaisankar, V. 3-Formylindole-based chitosan Schiff base polymer: Antioxidant and in vitro cytotoxicity studies on THP-1 cells. Carbohydrate Polymers,2022, 290, 119501. https://doi.org/10.1016/j.carbpol.2022.119501.
12. Ali, M. A.; Aswathy, K. A.; Munuswamy-Ramanujam, G.; Jaisankar, V. Pyridine and isoxazole substituted 3-formylindole-based chitosan Schiff base polymer: Antimicrobial, antioxidant and in vitro cytotoxicity studies on THP-1 cells. International Journal of Biological Macromolecules,2022, 225, 1575–1587. https://doi.org/10.1016/j.ijbiomac.2022.11.214.
13. Liu, X.; Dan, N.; Dan, W.; Gong, J. Feasibility study of the natural derived chitosan dialdehyde for chemical modification of collagen. International Journal of Biological Macromolecules,2015, 82, 989–997. https://doi.org/10.1016/j.ijbiomac.2015.11.015.
14. Sionkowska, A.; Kaczmarek, B.; Michalska, M.; Lewandowska, K.; Grabska, S. Preparation and characterization of collagen/chitosan/hyaluronic acid thin films for application in hair care cosmetics. Pure and Applied Chemistry,2017, 89 (12), 1829–1839. https://doi.org/10.1515/pac-2017-0314.
15. Lewandowska, K.; Furtos, G. Study of apatite layer formation on SBF-treated chitosan composite thin films. Polymer Testing,2018, 71, 173–181. https://doi.org/10.1016/j.polymertesting.2018.09.007.

16. Rashwan, A.K., Younis, H.A., Abdelshafy, A.M. et al. Plant starch extraction, modification, and green applications: a review. Environ Chem Lett 22, 2483–2530 (2024). https://doi.org/10.1007/s10311-024-01753-z
17. Mo, J., Rashwan, A.K., Osman, A.I. et al. Potential of Chinese Bayberry (Myrica rubra Sieb. et Zucc.) Fruit, Kernel, and Pomace as Promising Functional Ingredients for the Development of Food Products: A Comprehensive Review. Food Bioprocess Technol 17, 3506–3524 (2024). https://doi.org/10.1007/s11947-023-03313-9
18. Mostafa, M. A., Ismail, M. M., Morsy, J. M., Hassanin, H. M. & Abdelrazek, M. M. Synthesis, characterization, anticancer, and antioxidant activities of chitosan Schiff bases bearing quinolinone or pyranoquinolinone and their silver nanoparticles derivatives. Polym. Bull.(2022), https:// doi. org/ 10. 1007/ s00289- 022- 04238-7 .

HOW TO CITE: B. Deepan Kumar, Jaisankar V, Chitosan Based Schiff Base Polymer Derived from 2-Acetyl Phenothiazine : Synthesis, Characterization, Evaluation of Antimicrobial and Antioxidant Activities, Int. J. of Pharm. Sci., 2026, Vol 4, Issue 1, 2619-2635. https://doi.org/10.5281/zenodo.18351180